Inorganic Chemistry
Article

Inorg. Chem. **2009**, *48*, 6599–6603 **6599**
DOI: 10.1021/ic9005778

Separation of the Oxide and Halide Part in the Oxohalide $Fe_3Te_3O_{10}Cl$ Due to High Lewis Acidity of the Cations

Dong Zhang,[†] Mats Johnsson,*[,†] Helmuth Berger,[‡] Reinhard K. Kremer,[§] Dirk Wulferding,[∥] and Peter Lemmens[∥]

[†]*Department of Inorganic Chemistry, Stockholm University, S-106 91 Stockholm, Sweden,* [‡]*Institut de Physique de la Matiere Complexe, Ecole Polytechnique Fédérale de Lausanne (EPFL), CH-1015, Lausanne, Switzerland,* [§]*Max Planck Institute for Solid State Research, Heisenbergstrasse 1, D-70569 Stuttgart, Germany, and* [∥]*Institute for Condensed Matter Physics, TU Braunschweig, D-38106 Braunschweig, Germany*

Received March 24, 2009

A new iron tellurite halide $Fe_3Te_3O_{10}Cl$ has been identified that crystallizes in the monoclinic space group $P2_1/c$. The crystal structure comprises channels where the Cl ions and also the stereochemically active lone-pair electrons on Te^{4+} are located. The Cl-atoms rather act as counterions than being part of the covalent/ionic network. The magnetic susceptibility indicates antiferromagnetic ordering below $T_N \sim 100$ K with a marked splitting of the field cooled (fc) and the zero-field cooled (zfc) susceptibility at low magnetic fields; the splitting disappears at higher magnetic fields. Heat capacity measurements confirm the long-range ordering at below this temperature. Only moderate shifts are observed with Raman spectroscopy at the magnetic transition.

Introduction

A synthesis concept based on forming oxohalides comprising p-element cations having stereochemically active lone-pairs and transition metal cations has resulted in several new structurally low-dimensional compounds and even quantum spin compounds.[1−3] The lone-pair cations Te^{4+} and Sb^{3+} have mainly been utilized in these studies. The lone-pair electrons, E, occupy a non-bonding orbital that is stereochemically active and can therefore be regarded as an additional ligand completing the coordination polyhedron. Depending on their Lewis-acid strength different transition metal cations vary in between being chalcophile and halophile in an oxohalide environment. The high Lewis acidity of Fe^{3+} will allow for strong bonds to oxygen to form that force, for example, Te^{4+} to accept a halide ion as a ligand. This is the case in $FeTe_2O_5X$ (X = Cl, Br) in which Te^{4+} has a highly unusual $[TeO_2X]$ coordination.[2] However, in compounds containing a comparatively weaker Lewis acid, such as Cu^{2+}, the halide ions bond to the metal cation and not to Te^{4+}.[3] There are also examples in the literature of oxohalide compounds that do not contain transition metal cations and where the halide ions act as counterions in between layers of net positive charge made up of antimony oxide.[4]

The aim of this study was to further explore a system comprising a transition metal cation that is a strong Lewis acid in combination with Te^{4+} in an oxohalide environment with the goal of forming a new low-dimensional compound.

Experimental Section

Single crystals of $Fe_3Te_3O_{10}Cl$ have been grown by chemical vapor phase transport from a mixture of Fe_2O_3 (Alfa Aesar 99.99%), TeO_2 (Acros 99%) and $FeCl_3$ (Alfa Aesar 98%) in the molar ratio 1:6:1. The powder mixture was sealed in quartz tubes (40 mm in diameter, 250 mm in length) with HCl as transport gas for the crystal growth. The ampules were then placed in a two zone gradient furnace and heated by 50 °C/h to 470 °C. The optimum temperatures at the source and deposition zones for the growth of single crystals have been 470 and 400 °C, respectively. Each experimental run lasted for 350−450 h. Three different kinds of single crystals were observed in the ampules as follows: (1) in the charge zone, needles with a maximum size of $1 \times 1 \times 10$ mm^3 of red-brown $Fe_3Te_3O_{10}Cl$; (2) in the center of the ampule, platelets

*To whom correspondence should be addressed. E-mail: matsj@inorg.su.se.

(1) (a) Johnsson, M.; Törnroos, K. W.; Lemmens, P.; Millet, P. *Chem. Mater*. **2003**, *15*, 68–73. (b) Johnsson, M.; Lidin, S.; Törnroos, K. W.; Bürgi, H. -B.; Millet, P. *Angew. Chem*. **2004**, *116*, 4392–4395. (c) *Angew. Chem., Int. Ed.* **2004**, *43*, 4292−4295. (d) Mayerová, Z.; Johnsson, M.; Lidin, S. *Solid State Sci*. **2006**, *8*, 849–854. (e) Mayerová, Z.; Johnsson, M.; Lidin, S. *Angew. Chem*. **2006**, *118*, 5730–5734. (f) *Angew. Chem., Int. Ed*. **2006**, *45*, 5602−5606; (g) Hugonin, Z.; Johnsson, M.; Lidin, S.; Wulferding, D.; Lemmens, P.; Kremer, R. K. *J. Solid State Chem*. **2008**, *181*, 2776–2782.

(2) Becker, R.; Johnsson, M.; Kremer, R. K.; Klauss, H.-H.; Lemmens, P. *J. Am. Chem. Soc*. **2006**, *128*, 15469–15475.

(3) (a) Johnsson, M.; Törnroos, K. W.; Mila, F.; Millet, P. *Chem. Mater*. **2000**, *12*, 2853–2857. (b) Becker, R.; Johnsson, M.; Kremer, R.; Lemmens, P. *J. Solid State Chem*. **2005**, *178*, 2024–2029. (c) Takagi, R.; Johnsson, M.; Gnezdilov, V.; Kremer, R. K.; Brenig, W.; Lemmens, P. *Phys. Rev*. **2006**, *B74*, 014413.

(4) (a) Alonso, J. A. *J. Chem. Soc., Dalton Trans*. **1998**, *12*, 1947–1949. (b) Alonso, J. A.; Gutérrez-Puebla, E.; Jerez, A.; Monge, A.; Ruiz-Valero, C. *J. Chem. Soc., Dalton Trans*. **1985**, *8*, 1633–1635.

Published on Web 06/10/2009

with a maximum size of $10 \times 10 \times 1$ mm^3 of yellow-greenish $FeTe_2O_5Cl$; (3) a number of white single crystals of TeO_2 formed at the cold end. Attempts have been made to synthesize the compound from a stoichiometric mixture of the starting components and also the potential Br-analogue ($Fe_3Te_3O_{10}Br$), so far without success.

Thermal gravimetry analyses were done using a TG-DTA1600 (LABSYS) in oxygen atmosphere from room temperature to 1400 °C with the heating rate 10 °C/min.

Single-crystal X-ray data were collected at 293 K on an Oxford Diffraction Xcalibur3 diffractometer with use of graphite-monochromatized Mo Kα radiation, $\lambda = 0.71073$ Å. The intensities of the reflections were integrated using the software CrysAlis RED that also was used for the analytical absorption correction.[5] The structure was solved by direct methods using the program SHELXS97 and refined by full-matrix least-squares on F^2 using the program SHELXL97.[6] The lone-pair positions were calculated in geometrically idealized positions 1.25 Å away from the Te atoms in accordance with Galy et al.[7] The structural drawings are made with the program DIAMOND;[8] 12129 reflections, of which 1983 were unique, were collected in the region $4.12 < \theta < 26.37°$; space group $P2_1/c$; unit cell dimensions $a = 4.91880(10)$ Å, $b = 16.2572(3)$ Å, $c = 12.9323(2)$ Å, $\beta = 110.018(1)°$, $Z = 4$, $V = 971.67(3)$ Å^3. All atoms are refined with anisotropic temperature parameters. $R = 0.0203$ for 1783 reflections; $wR = 0.0473$, and $S = 1.193$ (the goodness of fit on F^2). Crystal data, details of structure determination, and bond lengths are given in Tables 1 and 2.

Magnetic susceptibilities of a powder sample (~75 mg) were measured as a function of magnetic field and temperature with a MPMS SQUID magnetometer (Quantum Design, 6325 Lusk Boulevard, San Diego). The measured susceptibilities were corrected for the diamagnetic contributions of the closed shells (-218×10^{-6} cm^3/mol; Fe^{3+}, -30×10^{-6} cm^3/mol; Te^{4+}, -42×10^{-6} cm^3/mol; O^{2-}, -12×10^{-6} cm^3/mol; Cl^-, -26×10^{-6} cm^3/mol)[9]. The high temperature susceptibility was corrected for a small trace of ferromagnetic impurities by a Honda−Owen type[10] extrapolation to $H \rightarrow \infty$ of several runs carried out at different magnetic fields ($1 \text{ T} \leq \mu_0 H \leq 7$ T).

The heat capacity of the same sample used for the susceptibility measurements was measured in a home-built automatic Nernst-type adiabatic calorimeter with a technique similar to that described in detail in ref 11. The sample was encapsulated in Duran glass flasks under ~900 mbar ^{4}He atmosphere to enable rapid thermal equilibration. A smaller sample of ~1 mg of selected crystals was measured in the temperature range $0.4 \text{ K} \leq T \leq 30$ K in a PPMS system employing the relaxation method. The heat capacities of the addenda (glass flask, Apiezon grease, sample platforms) were measured in separate runs and subtracted from the total heat capacities.

Raman scattering has been performed on individual single crystals in quasi-backscattering geometry using a laser power of 1 mW, a laser wavelength of 532 nm, and a cryostat with a temperature range from 3.5 to 300 K. Because of the large number of atoms in the unit cell and the low symmetry, a very large number of Raman active modes has been observed. The partial overlap of these modes makes a counting of modes and further symmetry analysis less meaningful. It has therefore been omitted.

Table 1. Crystal Data and Structure Refinement Parameters for $Fe_3Te_3O_{10}Cl$

empirical formula	$Fe_3Te_3O_{10}Cl$
formula weight	745.80
temperature (K)	293(2)
wavelength (Å)	0.71073
crystal system	monoclinic
space group	$P2_1/c$
a (Å)	4.91880(10)
b (Å)	16.2572(3)
c (Å)	12.9323 (2)
β (deg)	110.0180(10)
volume (Å ^{3})	971.67(3)
Z	4
density$_{calc}$, (g cm^{-3})	5.098
absorption coefficient (mm^{-1})	13.566
F(000)	1324
reflections collected	12129
independent reflections	1983 [R(int) = 0.0410]
data/restraints/parameters	1983/0/155
refinement method	full-matrix least-squares on F^2
goodness-of-fit on F^2	1.193
final R indices [$I > 2$sigma(I)][a]	$R_1 = 0.0189$, w$R_2 = 0.0468$
R indices (all data)	$R_1 = 0.0203$, w$R_2 = 0.0473$

[a] $R_1 = \sum||F_o| - |F_c||/\sum|F_o|$; $wR_2 = \{\sum w(F_o^2 - F_c^2)^2/\sum w(F_o^2)^2\}^{1/2}$.

Table 2. Selected Bond Lengths (Å) for $Fe_3Te_3O_{10}Cl$[a]

Te(1)−O(1)	1.8625(12)	Fe(1)−O(1)$^{\#2}$	1.9833(12)
Te(1)−O(3)	1.8790(10)	Fe(1)−O(10)$^{\#8}$	2.1046(11)
Te(1)−O(2)	1.9594(11)	Fe(1)−O(4)	2.1387(11)
Te(1)−Cl(1)$^{\#1}$	2.9136(5)	Fe(2)−O(7)	1.9692(9)
Te(2)−O(5)	1.8330(12)	Fe(2)−O(4)	2.0126(12)
Te(2)−O(6)	1.9247(10)	Fe(2)−O(2)	2.0145(12)
Te(2)−O(4)	1.9489(12)	Fe(2)−O(6)$^{\#3}$	2.0259(10)
Te(3)−O(9)	1.8233(11)	Fe(2)−O(8)	2.0458(12)
Te(3)−O(8)	1.9659(10)	Fe(2)−O(7)$^{\#6}$	2.0745(11)
Te(3)−O(10)$^{\#3}$	1.9740(12)	Fe(3)−O(7)$^{\#7}$	1.9688(9)
Te(3)−O(3)$^{\#4}$	2.4109(11)	Fe(3)−O(10)	1.9724(12)
Te(3)−Cl(1)$^{\#5}$	2.8492(5)	Fe(3)−O(2)$^{\#6}$	1.9941(12)
Fe(1)−O(9)$^{\#8}$	1.9391(12)	Fe(3)−O(8)	2.0353(9)
Fe(1)−O(5)$^{\#3}$	1.9530(11)	Fe(3)−O(6)	2.1055(12)
Fe(1)−O(3)	1.9693(12)	Fe(3)−O(7)	2.1063(11)

[a] Note: symmetry transformations used to generate equivalent atoms are given below. $^{\#1}$ $x, -y+1/2, z+1/2$. $^{\#2}$ $x, -y+1/2, z-1/2$. $^{\#3}$ $x-1, y, z$. $^{\#4}$ $-x, y+1/2, -z+3/2$. $^{\#5}$ $-x+1, -y+1, -z+1$. $^{\#6}$ $-x+1, -y+1, -z+2$. $^{\#7}$ $-x+2, -y+1, -z+2$. $^{\#8}$ $-x+1, y-1/2, -z+3/2$.

Results and Discussion

Crystal Structure. The new iron tellurite halide $Fe_3Te_3O_{10}Cl$ crystallizes in the monoclinic space group $P2_1/c$. The unit cell is $a = 4.91880(10)$ Å, $b = 16.2572(3)$ Å, $c = 12.9323(2)$ Å, $\beta = 110.0180(10)°$. EDS analysis confirms the stoichiometry of atoms heavier than oxygen. Bond valence sum (BVS) calculations have been performed according to Brown and Altermatt[12] and the distances for the primary bonding sphere for the ions have been defined as in ref 2. The R_0 values used for these calculations are R_0(Te−O) = 1.977,[12] R_0(Te−Cl) = 2.37,[13] R_0(Fe−O) = 1.765.[14]

The crystal structure is a 3D network with channels along [100]. The Cl^- atoms are located in these channels where also the stereochemically active lone-pairs of the Te^{4+} ions, designated E, are located, see Figure 1.

(5) *CrysAlisCCD and CrysAlisRED*; Oxford Diffraction Ltd.: Abingdon, Oxfordshire, England, 2006.
(6) Sheldrick, G. M. *Acta Crystallogr.* **2008**, *A64*, 112–122.
(7) Galy, J.; Meunier, G.; Andersson, S.; Åström, A. *J. Solid State Chem.* **1975**, *13*, 142–159.
(8) *DIAMOND*; Bergerhoff, G., Bonn, Germany, 1996.
(9) Selwood, P. W. *Magnetochemistry*, 2nd ed.; Interscience: New York, 1956; p 447.
(10) Honda, K. *Ann. Phys. (Leipzig)*. **1910**, *32*, 1027–1063.
(11) (a) Gmelin, E. *Thermochim. Acta* **1979**, *29*, 1–39. (b) Gmelin, E.; Rödhammer, P. *J. Phys. E (Sci. Instrum.)*. **1981**, *14*, 223–228. (c) Gmelin, E.; Ripka, K. *Cryogenics*. **1981**, *21*, 117–118.
(12) Brown, I. D.; Altermatt, D. *Acta Crystallogr.* **1985**, *B41*, 244–247.
(13) Brese, N. E. *Acta Crystallogr.* **1991**, *B47*, 192–197.
(14) Liu, W.; Thorp, H. H. *Inorg. Chem.* **1993**, *32*, 4102–4105.

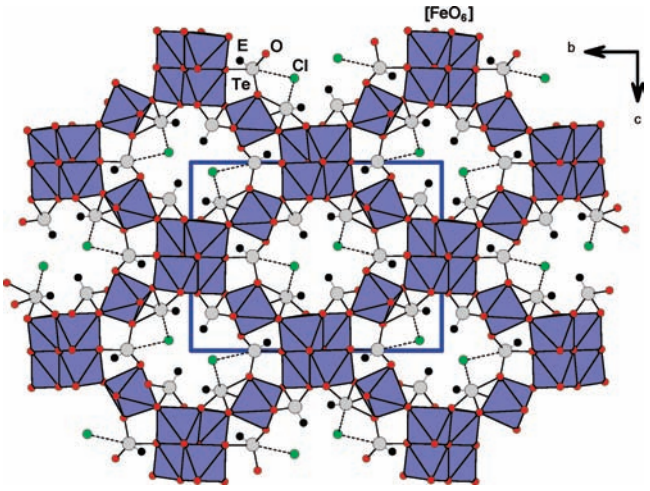

Figure 1. Crystal structure of $Fe_3Te_3O_{10}Cl$ seen along [100]. The weak Te−Cl bonds are dotted.

There are three crystallographically different Fe^{3+} positions; all of them have distorted [FeO_6] octahedral coordinations. Two [Fe(2)O_6] and two [Fe(3)O_6] octahedra are connected by edge sharing to form $[Fe_4O_{16}]^{-20}$ units that further connect to form chains extending along [100]. The chains are linked via Fe−O−Fe corner sharing by the [Fe(1)O_6] octahedra to form the 3D network. The four Fe atoms in one $[Fe_4O_{16}]^{-20}$ unit form a distorted tetrahedron; these Fe-tetrahedrons connect to form chains by edge sharing, see Figure 2. The iron atoms are coordinated by only oxygen and no chlorine as is also the case in, for example, the oxohalide $FeTe_2O_5X$ (X = Cl, Br) [2] while Cu^{2+} or Ni^{2+} [1,3] tend to bond to both oxygen and halide ions and Cu^{+} to only halide ions [1]. The Lewis acidity and the softness of the metal cations thus have significant influence on the resulting crystal structure because of their bonding preferences. There are three crystallographically different Te^{4+} cations, which all have one-sided coordination because of the presence of the stereochemically active lone-pair electrons. Te(1) has a distorted [Te(1)O_3ClE] trigonal bipyramidal coordination. Te(2) coordinates three oxygens forming a [Te(2)O_3E] tetrahedron. Te(3) has a [Te(3)O_{3+1}ClE] distorted square planar bipyramidal coordination with three shorter and one longer Te−O bond distances. The Te(1)−Cl(1) and the Te(3)−Cl(1) distances are 2.9136(5) and 2.8492(5) Å respectively, and such long distances are at the border of what can be considered as belonging to the primary coordination sphere of Te^{4+}. The [Te(1)O_3ClE] and [Te-(3)O_{3+1}ClE] polyhedra form pairs by connecting to each other via a common oxygen Te(1)−O(3)−Te(3); those pairs further link to a similar pair via a common Cl; Te-(1)−Cl(1)−Te(3) to build up a chain in the crystal structure; the [Te(2)O_3E] polyhedra do not connect to the other Te-polyhedra. The Te-polyhedra bond further to the network of [FeO_6] octahedra by corner sharing; [Te(3)O_4ClE] also has a common corner with [Fe(1)O_6].

BVS calculations give values close to the expected valences for all ions except for the chlorine; the three Te get values of 3.71−4.13 supporting that they all are Te^{4+}, the three Fe get values in the range 2.97−3.11 supporting that they all are Fe^{3+}. The chlorine gets a value of 0.50 vu indicating that it rather takes the role of a counterion than

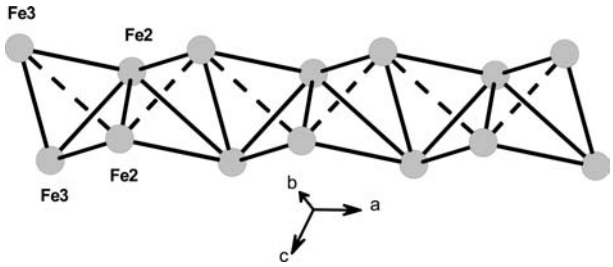

Figure 2. Fe2 and Fe3 atoms form chains of edge sharing distorted tetrahedra that extend along [100].

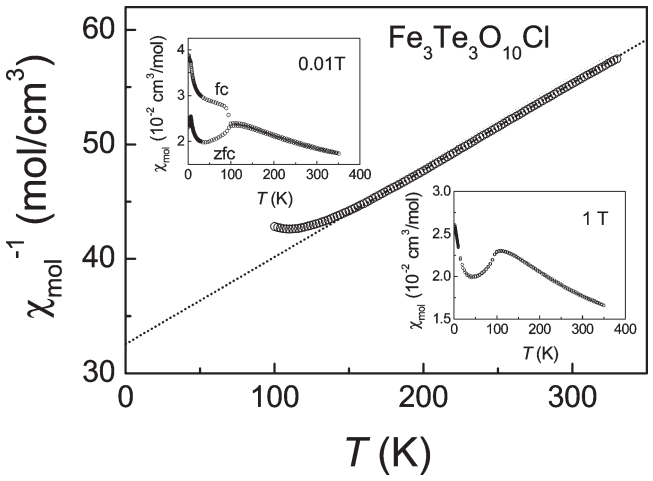

Figure 3. Magnetic susceptibility of $Fe_3Te_3O_{10}Cl$ corrected for the diamagnetic contributions from the closed shells and a trace of a ferromagnetic impurity (see text). The dotted line corresponds to a Curie−Weiss law assuming an effective magnetic moment of 5.92 μ_B per Fe^{3+} ion and a Curie−Weiss temperature of θ = −434 K. The insets display the magnetic susceptibilities measured in fields of 0.01 and 1 T. The marked splitting between the field-cooled (fc) and the zero-field-cooled (zfc) susceptibility below T_N disappears in larger magnetic fields where fc and zfc susceptibilities coincide within error bars.

being fully integrated in the covalent/ionic network. If all Te−Cl distances up to 4.5 Å are taken into account in the BVS calculations then the valence for Cl reaches 0.73 vu; however, this is still far from the expected value of 1. Underbonded halides are common in oxohalides and have been reported, for example, in the other iron tellurium oxohalides described, $FeTe_2O_5X$ (X = Cl, Br) [2], $Fe_8Te_{12}O_{32}Cl_3Br_3$, and $Fe_5Te_6O_{18}Cl_2$.[15] Thermal gravimetry gives that $Fe_3Te_3O_{10}Cl$ is stable up to 620 °C and then starts to decompose in several steps; PXRD gives that it is mainly Fe_2O_3 that is left at 1400 °C.

Magnetic Properties. The magnetic susceptibility of $Fe_3Te_3O_{10}Cl$ indicates antiferromagnetic ordering below $T_N \sim 100$ K with a marked splitting of the field cooled (fc) and the zero-field cooled (zfc) susceptibility possibly indicating a spin canted arrangement of the magnetic moments in the ordered state, see Figure 3. The marked splitting disappears at larger fields, and fc and zfc susceptibilities are identical. Above ~175 K, the susceptibility follows a Curie−Weiss law with a Curie−Weiss temperature of −434(2) K and a Curie constant of 3 × 4.38 cm^3 K/mol corresponding to an effective magnetic moment of 5.92 μ_B per Fe^{3+} ion, in best agreement with

(15) Becker, R.; Johnsson, M. *J. Solid State Chem.* **2007**, *180*, 1750–1758.

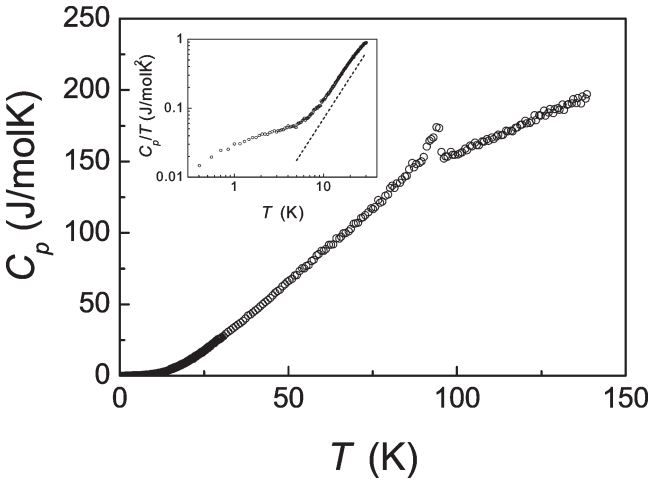

Figure 4. Heat capacity C_p of $Fe_3Te_3O_{10}Cl$. The inset shows C_p/T vs T and reveals the deviation from a power law $C_p \sim T^3$ below ~8 K. The broad feature contains an entropy of 0.15 J/mol·K corresponding to 0.01 mol of $S = 5/2$ magnetic entities.

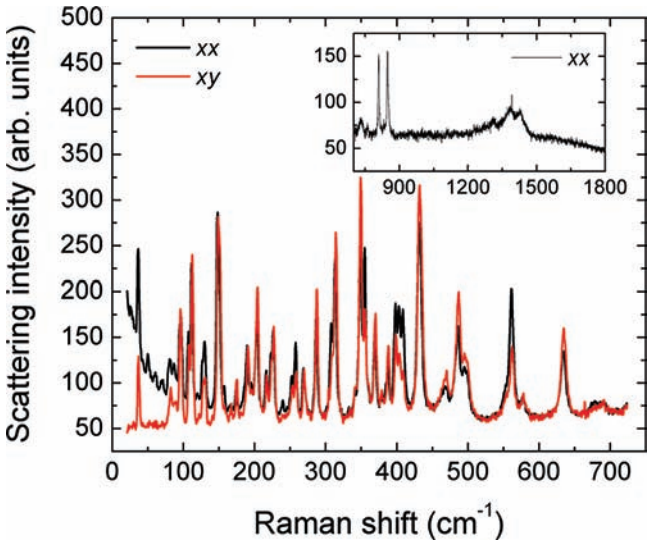

Figure 5. Raman spectra of $Fe_3Te_3O_{10}Cl$ at $T = 3.5$ K in parallel (xx) and crossed (xy) polarization. Inset: High-frequency regime.

the effective moment expected for a $3d^5$ configuration with spin-only $S = 5/2$ and a g-factor near 2. The upturn at low temperatures and the peak in the 0.01 T zfc, respectively, and the shoulder in the fc susceptibility seen at ~8 K may be attributed to a small, yet unidentified, paramagnetic impurity (0.7% of $S = 5/2$ magnetic entities) which undergoes magnetic ordering near 8 K. Deviations of the magnetic susceptibility between 200 K and T_N indicate an extended critical regime possibly because of afm short-range ordering above T_N.

The heat capacity of $Fe_3Te_3O_{10}Cl$ shows a λ-type anomaly at 95(1) K confirming long-range magnetic ordering found in the magnetic susceptibility measurement, see Figure 4. Below ~8 K the heat capacity deviates from a T^3 power law expected for the spin-wave contributions of a three-dimensional antiferromagnet. A broad feature appears which contains an entropy of ~0.15 J/mol·K corresponding to the entropy of ~1% mol of $S = 5/2$ magnetic entities, in good agreement with the concentration of paramagnetic impurities derived from the magnetic susceptibility analysis.

The entropy contained in the λ-anomaly at T_N amounts to ~5(1) J/mol·K which represents only ≈10% of the total magnetic entropy available in the system, $3 \times R \ln 6 \approx 45$ J/mol·K. The remaining entropy must apparently be removed in short-range ordering processes above T_N. In line with the susceptibility experiments this finding reflects the structural properties with the marked chain-like arrangement of the Fe(2) and Fe(3) atoms leading to a larger superexchange interaction within the tetrahedral chains than between them. Short range ordering contributions to the heat capacity of low-dimensional magnetic systems have a shape of a very broad Schottky-type anomaly[16] and therefore are difficult to separate from the total heat capacity since at higher temperatures the lattice contributions to the heat capacity dominate the total heat capacity.

We observe Raman lines in the frequency range from 40 to 880 cm^{-1} and attribute these to phonon modes, see Figure 5. Similar to observations in other lone-pair systems the observed modes group as function of frequency pointing to characteristic frequencies for rotational bending and local distortional modes.[17] These groups are centered around 126, 220, 380, and 490 cm^{-1}. At low temperatures ($T = 3.5$ K) in (xx) light polarization an additional low frequency tail is observed. In contrast, for (xy) polarization the background is very flat. The former continuum is a candidate for magnetic scattering[17] and can be compared to the observation in Cu dimer systems, $TlCuCl_3$ and $KCuCl_3$.[18,19] Centered at about 1310, 1385, and 1427 cm^{-1}, broad and overlapping maxima are observed. At approximately half of these frequencies intensive sharp modes exist at 562, 635, 690, 809, and 848 cm^{-1}. Therefore, we attribute the broad maxima to two-phonon processes. Similar maxima exist at 732 and 761 cm^{-1} with corresponding original phonon modes at 350, 356, 370, 389, 399 cm^{-1}. The observation of multiphonon scattering is related to anharmonic contributions to the lattice potential expected for the given channel structures and lone pair ions. The latter also contribute to the large overall Raman scattering intensity via their large electronic polarizability. We have searched for changes related to the magnetic transition but found only moderate shifts, enhancements of intensity, and peak splitting of phonons in the frequency range 100−300 cm^{-1}.

Conclusion

The new compound $Fe_3Te_3O_{10}Cl$ has a 3D oxide network with the Cl^- atoms and the stereochemically active lone-pairs on Te^{4+} located in channels in the structure. The Cl^- atoms act more as counterions rather than being part of the covalent/ionic network. The magnetic susceptibility indicates antiferro-magnetic ordering below T_N ~100 K possibly due

(16) de Jongh, L. J.; Miedema, A. R. *Adv. Phys.* **1974**, *23*, 1.

(17) Lemmens, P.; Güntherodt, G.; Gros, C. *Physics Rep.* **2003**, *375*, 1–103.

(18) Choi, K.-Y.; Güntherodt, G.; Oosawa, A.; Tanaka, H.; Lemmens, P. *Phys. Rev.* **2003**, *B 68*, 174412/1–174412/6.

(19) Choi, K.-Y.; Oosawa, A.; Tanaka, H; Lemmens, P. *Phys. Rev.* **2005**, *B 72*, 024451/1–024451/5.

to a canted magnetic structure. Heat capacity measurements confirm the long-range ordering at below this temperature. Only moderate shifts are observed with Raman spectroscopy at the magnetic transition. An interesting future experiment will be to search for oxohalide host−guest compounds by combining transition metal cations with strong and weak Lewis acidity, that is, combining chalcophile and halophile metal cations in an oxohalide environment.

Acknowledgment. This work has been carried out through financial support from the Swedish Research Council, the Swiss National Science Foundation (SNSF), the German Science Foundation (DFG), and the scientific program Highly Frustrated Magnetism supported by the European Science Foundation (ESF).

Supporting Information Available: Photograph showing the synthesis product of red crystals of $Fe_3Te_3O_{10}Cl$, experimental and simulated Powder X-ray diffraction pattern, thermal gravimetric measurement, results from energy-dispersive spectrometry (EDS) analysis of the chemical composition of synthesized crystals, and results from BVS calculations. This material is available free of charge via the Internet at http://pubs.acs.org. Further details on the crystal structural investigations may be obtained from the Fachinformationszentrum Karlsruhe, Abt. PROKA, 76344 Eggenstein-Leopoldshafen, Germany (fax +49−7247−808−666; E-mail: crysdata@fiz-karlsruhe.de) on quoting the depository number CSD-419697.